processes

MDPI

Article

Multi-Objective Optimisation of Injection Moulding Process for Dashboard Using Genetic Algorithm and Type-2 Fuzzy Neural Network

Mohammad Reza Chalak Qazani [1], Mehdi Moayyedian [2,*], Parisa Jourabchi Amirkhizi [3], Mohsen Hedayati-Dezfooli [4], Ahmed Abdalmonem [2], Ahmad Alsmadi [2] and Furqan Alam [1]

1 Faculty of Computing and Information Technology, Sohar University, Sohar 311, Oman; mqazani@su.edu.om (M.R.C.Q.); falam@su.edu.om (F.A.)
2 College of Engineering and Technology, American University of the Middle East, Egaila 54200, Kuwait; ahmed.abdalmonem@aum.edu.kw (A.A.); ahmad.alsmadi@aum.edu.kw (A.A.)
3 Design Faculty, Tabriz Islamic Art University, Tabriz 5164736931, Iran; p.jourabchi@tabriziau.ac.ir
4 Department of Mechanical Engineering, College of Engineering and Technology, University of Doha for Science and Technology, Arab League St., Doha P.O. Box 24449, Qatar; mohsen.hedayati@udst.edu.qa
* Correspondence: mehdi.moayyedian@aum.edu.kw

Abstract: This study examines the use of injection moulding to evaluate mechanical properties in plastic products, such as shear and residual stresses. Key process variables like melt temperature, mould temperature, hold pressure duration, and pure hold duration are meticulously chosen for study. A full factorial experiment design is utilised to determine the best settings. These variables notably influence the end product's physical and mechanical properties. Computational techniques, like the finite element method, are used to analyse behaviours based on varied input parameters. A CAD model of a dashboard part is incorporated into a finite element analysis to measure shear and residual stresses. Four specific parameters from the injection moulding process are subjected to an in-depth experimental design. It is worth noting that the injection moulding process does not incorporate a type-2 fuzzy neural network (T2FNN). However, in this particular investigation, T2FNN was employed to replicate the mechanical stress model associated with dashboard injection moulding. Its purpose was to estimate shear and residual stress levels. Additionally, the multi-objective genetic algorithm (MOGA) was utilised to extract the most optimal parameters for the injection moulding process, aiming to minimise shear and residual stress and thereby increase the resistance of the final product. The proposed model was developed and implemented using MATLAB software. A Pareto front was derived from the MOGA by employing the T2FNN within the process, identifying fourteen optimal solutions.

Keywords: injection moulding; shear/residual stress; type-2 fuzzy neural network; multi-objective optimisation; genetic algorithm

check for updates

Citation: Qazani, M.R.C.; Moayyedian, M.; Amirkhizi, P.J.; Hedayati-Dezfooli, M.; Abdalmonem, A.; Alsmadi, A.; Alam, F. Multi-Objective Optimisation of Injection Moulding Process for Dashboard Using Genetic Algorithm and Type-2 Fuzzy Neural Network. *Processes* **2024**, *12*, 1163. https://doi.org/10.3390/pr12061163

Academic Editors: Jiaqiang E and Roberto Pisano

Received: 22 April 2024
Revised: 28 May 2024
Accepted: 3 June 2024
Published: 5 June 2024

Copyright: © 2024 by the authors. Licensee MDPI, Basel, Switzerland. This article is an open access article distributed under the terms and conditions of the Creative Commons Attribution (CC BY) license (https://creativecommons.org/licenses/by/4.0/).

1. Introduction

The process of plastic injection moulding encompasses multiple steps. First, polymer substances and additives are introduced into the machine's heating system. After injecting the melted polymer into the mould cavity during filling, additional polymer melt is supplied under increased pressure during the packing phase to compensate for shrinkage. Subsequently, cooling occurs until the component solidifies. Finally, the mould opens, and the plastic component is extracted using ejector pins, marking the completion of one cycle of the process, which then begins anew, as illustrated in Figure 1 [1–3].

The mechanical properties of moulded items can be unpredictable. Experienced operators often accumulate vast knowledge to discern the best process variables. There is a distinct link between these variables and the mechanical properties of the moulded component in injection moulding. Inadequate adjustments can result in different mechanical

characteristics, notably shear and residual stress [4]. In injection moulding, shear and residual stresses are frequently examined. Shear stress arises from shear forces, a force vector component aligned with the material's cross-section, creating internal tension [5]. Additionally, even after the original stress source is gone, residual stresses can remain in a solid material [6], which can either be beneficial or detrimental.

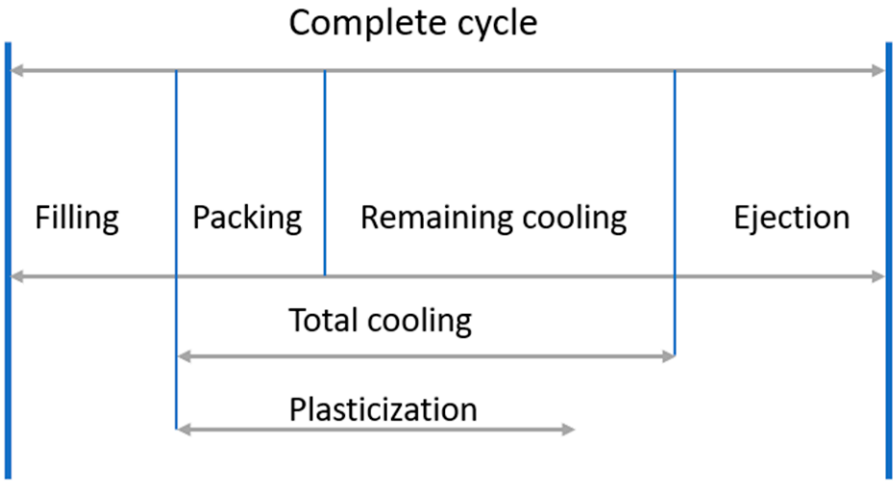

Figure 1. Injection moulding cycle.

Schwetz et al. [7] investigated the mechanical properties of the B4C–C ceramics in the injection moulding process. Torres et al. [8] investigated the influence of different process parameters of injection moulding on the thermal and mechanical properties of the final product. Ozcelik et al. [9] investigated the injection moulding process parameters and mould material influences on the final product of injection moulding using ABS materials. Kuzmanović et al. [10] studied the influence of moulding temperature on the mechanical properties of PP/PET blends and microfibrillar composites. Recently, Krantz et al. [11] investigated pressure-controlled injection moulding on recycled high-density polyethylene's mechanical properties and embodied energy.

Chin and Wong [12] introduced a knowledge-based system for efficient plastic product design, including material selection and injection mould feature generation. Kenig et al. [13] demonstrated the accurate prediction of plastic mechanical properties using Artificial Neural Networks, advancing potential self-taught control in injection moulding. Tan and Tang [14] introduced a learning-enhanced PI control for injection moulding machines, combining feedback and feedforward with an iterative learning algorithm for improved performance and disturbance compensation. Abbasalizadeh et al. [15] investigated the impact of injection moulding parameters on polymer shrinkage. They emphasised the significant influence of material crystallinity and flow direction on the shrinkage phenomenon. By employing the Taguchi approach, they identified optimal conditions for minimising shrinkage. Abdul et al. [16] proposed combining a multilayer perceptron model and the Taguchi approach to predict and minimise part shrinkage in injection moulding. Their approach not only improved the quality of the final product but also facilitated the setup process for moulding.

Similarly, Song et al. [17] developed a hybrid model incorporating a genetic algorithm, a multilayer perceptron, and support vector regression. This model aimed to optimise design parameters and accurately predict warpage and volume shrinkage in the injection moulding process. Gao et al. [18] introduced machine learning methods such as the multilayer perceptron, support vector regression, and kernel ridge to design conformal cooling channels in injection moulding. Their approach reduced temperature variance and enhanced cooling quality compared to conventional designs. Jung et al. [19] evaluated various machine learning techniques to assess their effectiveness in predicting injection moulding quality. Lastly, Uğuroğlu [20] introduced a real-time application for plastic

injection moulding machines. Their approach involved using machine learning methods such as k-nearest neighbour, random forest, logistic regression, and multilayer perceptron to enhance the performance and functionality of the machines.

In recent times, considerable attention has been devoted to enhancing the effectiveness of process parameters within injection moulding. Párizs et al. [21] undertook a comparative analysis of diverse machine learning methods to predict the quality of multi-cavity injection moulding. Their findings revealed that the decision tree model outperformed others, achieving an impressive accuracy rate exceeding 90%. Similarly, Ke and Huang [22] introduced an optimised multilayer perceptron model featuring a Sigmoid activation function and a learning rate of 0.1. Remarkably, this model achieved a remarkable accuracy of 95.8%. Moayyedian et al. [23] developed a computationally efficient model employing genetic programming techniques to optimise injection moulding parameters in another study. Their approach yielded significantly lower mean squared error (MSE) values than alternative methods like support vector regression, decision trees, and multilayer perceptron. Demonstrating their versatility, Gim et al. [24] utilised transfer learning techniques to optimise process parameters for achieving superior surface quality in injection moulding. By training a multi-task multilayer perceptron model on data collected from the original production site and subsequently transferring it to a new site, they not only improved surface gloss prediction but also reduced the size of the dataset. Consequently, this approach facilitated the efficient production of high-quality moulded parts. Fernández-León et al. [25] introduced a surrogate model using an encoder–decoder approach for simulating dual-phase flow in liquid moulding. Novel loss functions and sampling strategies enhance accuracy and efficiency, improving the predictions of pressure, front flow, and structural properties. Zhang et al. [26] introduced an IDD-Net, a deep learning method for industrial defect detection. It addresses diversity, similarity, and scale challenges using a novel local-global feature network and a three-layer feature aggregation network with a specialised IoU loss. Experimental results demonstrate superior performance on various datasets and real industrial applications.

Also, Moayyedian, Dinc, and Mamedov (2021) conducted research on optimising injection moulding processes to minimise defects in plastic parts. They utilised Artificial Neural Networks, Taguchi Techniques, and Analytic Hierarchy Process to determine optimal parameters. Finite Element Analysis validated the parameters, showing the best quality with specific settings like filling time, cooling time, pressure-holding time, and melt temperature. The study highlighted filling time as the most influential factor and concluded with a 1.5% margin of error due to uncontrollable process parameters [27].

The primary objective of this study is to develop a highly efficient machine-learning approach for accurately determining the shear and residual stress within the injection moulding process of plastic products. Notably, the utilisation of a type-2 fuzzy neural network (T2FNN) for this purpose is a novel contribution, as previous investigations have primarily focused on other methodologies such as knowledge-based systems [12,13], linear regression [19,20], multilayer perceptron [14,16–18,20,22,23], support vector regression [17–19,23], random forest [19,20], decision tree [19,21,23], k-nearest neighbour [20,21], genetic programming [23], deep learning [25,26], and transfer learning [24]. These earlier studies have successfully extracted models with the ability to emulate the behaviour of the injection moulding process. Nevertheless, the specific application of a T2FNN within this domain has not been explored, thus signifying this current investigation's novelty and innovative nature. Consequently, a T2FNN has been employed in this study as a key component of the research methodology. The versatility of this approach becomes evident when considering its ability to effectively manage uncertainty within a dynamic optimal learning framework. Furthermore, the inherent strength of this method lies in its exceptional estimation capabilities, enabling the precise identification of complex systems. It is important to note that, in contrast to type-1 fuzzy neural networks, the secondary membership in type-2 systems is expressed as a fuzzy set. As a result, type-2 fuzzy sys-

tems possess additional freedom, enhancing their adaptability and flexibility in handling diverse scenarios.

Acquiring the necessary dataset for training/testing purposes of machine learning methods can be accomplished through two primary approaches: experimental setups and finite element simulation. Conducting experimental studies is not only costly but also time-consuming. Conversely, finite element simulation offers a more convenient alternative, allowing for easier dataset extraction without actual experiments. It is worth highlighting that in this particular study, the required dataset for training/testing of the machine-learning method was obtained through finite element simulation. Various inputs were selected, including melt temperature, mould temperature, pressure holding time, and pure holding time. Applying a type-2 fuzzy model in this study enhances the model's accuracy, specifically in handling the uncertainties inherent in the process.

Moreover, the integration of neural networks and fuzzy systems, forming the T2FNN, significantly reduces the training and testing duration of the system, making it highly suitable for online applications. Notably, this is the first instance in which T2FNN has been utilised for modelling the injection moulding procedure. Additionally, the extracted T2FNN model is incorporated into the multi-objective genetic algorithm (MOGA) to calculate the optimal solution of the injection moulding process, resulting in reduced shear and residual stress, ultimately minimizing internal defects. It is essential to acknowledge that MOGA is a pioneering technique in multi-objective optimisation, proficient in determining optimal parameters for complex systems across various sectors.

Section 2 comprehensively examines the injection moulding process, specifically on producing intricate dashboard components. Furthermore, this section outlines the methodology for acquiring the necessary datasets, utilizing the finite element simulation environment. Moving forward to Section 3, a detailed explanation regarding the innovative approach incorporating the combined utilisation of T2FNN and MOGA is provided. Section 4 of this manuscript offers a comprehensive comparative analysis and thought-provoking discussion, delving into the outcomes extracted through the developed model implemented within the MATLAB framework (MATLAB R2017B). Finally, in Section 6, the study reaches its culmination as key conclusions derived from the research are summarised and highlighted.

2. Injection-Moulding Process for Dashboard

Shear and residual stress are the main important mechanical properties of injection moulding. In injection moulding, shear stress is the tension created within the molten polymer when it navigates through the mould. As the liquefied plastic is pushed into the mould's channels and cavities, it encounters resistance, leading to shearing forces. This stress is born out of the velocity differences, or the change in flow speed, within the molten polymer's path. The molten plastic layers near the mould boundaries tend to move slower than the central layers because of the friction against the mould surfaces. Such variation in movement between these layers is what produces shear stress.

The literature review pinpointed shear and residual stresses for the comprehensive examination. A full-factorial design is applied to determine the paramount factors impacting the selected plastic component's mechanical properties for optimal design. Figure 2 presents the dashboard's modelling, with (a) depicting its solid form. The simulation methodology leverages finite element analysis and SOLIDWORKS Plastic. The cooling framework for the plastic component is conceived using a cool pipe model, integrating the cooling channels into the mould's solid depiction. In this cyclical approach, the fluctuating thermal profiles of the heated mould and cavity are calculated through the cool solver. Ambient temperature serves as a reference for the initial heating. Finite element analysis is instrumental in the simulation, ensuring the analytical results' integrity and precision. Within this analysis, surface meshes adopt triangular configurations aligning with the specimen's geometric nuances, as illustrated in Figure 2b. After assessing multiple dimensions, a 1 mm surface mesh size is chosen for the injection segment.

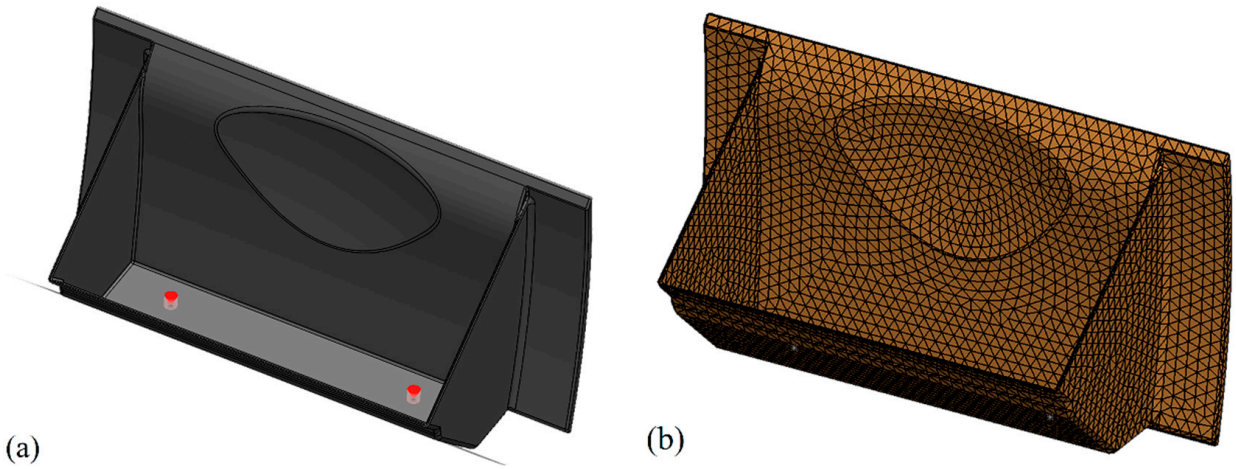

Figure 2. (**a**) Solid modelling of the dashboard; (**b**) the meshed model with triangle meshes.

Shear and residual stress are crucial for product quality. Elevated shear stress during molding can cause internal flaws and weaken bonds, reducing resilience and durability. Residual stresses post-cooling can lead to warping or cracking, compromising structural integrity. Additionally, dimensional discrepancies and surface imperfections affect function, aesthetics, and visual appeal. Long-term performance may suffer due to stress-induced material degradation or instability. Effective stress management is vital for ensuring product quality and longevity across industries [1,28].

This study delves into diverse process parameters, such as pure cooling duration, melt temperature, mould temperature, and hold pressure duration. The viscosity of the polymer melt is influenced by melt temperature, where higher temperatures typically result in lower viscosity, potentially decreasing shear stress during filling. Mold temperature, on the other hand, affects the rate of cooling and polymer crystallisation, influencing the residual stresses present in the final part. Extended pressure holding times facilitate better mold cavity packing, which may decrease voids and enhance part density, thus affecting shear stress. Similarly, prolonged cooling times promote controlled polymer solidification, potentially reducing residual stresses by minimising thermal gradients and internal stress accumulation [1,28]. Achieving optimal results necessitates balancing these parameters to minimise both shear and residual stresses while ensuring the desired properties and dimensional accuracy of the injection-molded plastic parts. These parameters undergo examination at varying levels, with melt temperature—identified as the most critical parameter—assessed at five distinct levels. In comparison, pure cooling time is evaluated at three levels. Simulation-based determinations ascertain each parameter's lowest and highest efficacious thresholds and the necessary intermediate levels. Acrylonitrile Butadiene Styrene (ABS) has been chosen as the focus material for this research. Generic ABS (Acrylonitrile Butadiene Styrene) is a favored choice among manufacturers for car glove boxes because of its robustness, resistance to impact, and heat, rendering it well-suited for the rigors of automotive interiors. ABS boasts dimensional stability across different temperature and humidity conditions, ensuring a snug fit of the glove box over its lifespan. Its versatility in molding intricate shapes enables the creation of designs meeting both functional and aesthetic requirements. In comparison to alternative plastics, ABS offers a harmonious blend of strength, impact resistance, heat resilience, and mouldability, solidifying its position as a premier option for automotive components such as glove boxes. Given the many parameters and associated levels detailed in Table 1, 180 simulations were performed utilizing SolidWorks Plastics.

Table 1. The selected parameters and their levels.

Parameters	L1	L2	L3	L4	L5
Melt temperature T_1 (°C)	200	215	230	255	280
Mould temperature T_2 (°C)	25	50	65	80	-
Pressure holding time t_1 (s)	10	20	30	-	-
Pure cooling time t_2 (s)	60	80	100	-	-

3. Methodology

This section's focal point lies in the proposed methodology, which revolves around integrating T2FNN and MOGA. A comprehensive investigation is undertaken, employing a full factorial analysis of the injection moulding process. This study embraces the power of the finite element simulation environment to capture the system's outputs, namely internal shear and residual stress, contingent upon a range of inputs: melt temperature, mould temperature, pressure holding time, and pure holding time. The subsequent step entails the utilisation of T2FNN to derive a surrogate model that faithfully emulates the behaviour exhibited by the injection moulding process. Concurrently, MOGA comes into play, extracting the optimal process parameters for the injection moulding machine. Crucially, the surrogate model extracted through T2FNN finds its place within the objective function of MOGA, fuelling its efficacy. In the ultimate stage, the obtained results from MOGA, manifesting as the Pareto front distribution of optimal solutions, are subjected to validation through the finite element simulation. This crucial step aims to increase the model's performance by presenting real-world examples where it excels in handling complex parts.

The proposed framework is visualised in Figure 3, presenting a concise representation of the innovative approach. This methodology unveils its true potential by comprising two pivotal steps. In the initial phase, emphasis is placed on training and extracting the T2FNN. Leveraging the invaluable datasets acquired from the preceding section, two distinct T2FNN models are developed, each catering to the prediction of specific outputs: maximum internal shear (T2FNN-Shear) and residual stress (T2FNN-Residual). Transitioning to the subsequent step, the utilisation of MOGA comes into play. This powerful algorithm takes centre stage, extracting the optimal process parameters. The primary objective is to minimise internal shear, residual stress, and defects, effectively enhancing the overall quality of the plastic parts. Notably, the raw datasets cannot be directly fed into the algorithm, which would compromise the model's accuracy. Hence, we delve into the importance of data preprocessing, which is extensively discussed in the initial subsection of this section. Through this preprocessing stage, we ensure the fidelity and reliability of the subsequent MOGA and T2FNN components. The following subsection provides a comprehensive breakdown of the MOGA and T2FNN techniques. This hybrid model serves as the key catalyst, facilitating the extraction of optimal process parameters within the injection moulding procedure of plastic parts.

3.1. Preprocessing

The dataset undergoes a crucial preprocessing stage to enhance the network's accuracy, aimed at mitigating the system's complexity. The process commences by removing out-of-range data, as these entries significantly impede the network's precision. Subsequently, normalisation takes centre stage, facilitating the allocation of mean and standard deviation values within a rational range. By achieving this, the system's complexity is effectively reduced, streamlining the network's operations. The calculations involved in this normalisation process are as follows:

$$n_{x_i} = \frac{x_i - \underline{x}}{\overline{x} - \underline{x}} \tag{1}$$

where $\overline{x}$ and $\underline{x}$ are the maximum and minimum values of the dataset. Additionally, let x_i represent the raw data at the ith position while n_{x_i} symbolises the corresponding normalised data. The normalised values are constrained within the interval [0, 1]. Acknowledging that the normalisation procedure is conducted independently for input and output data is vital.

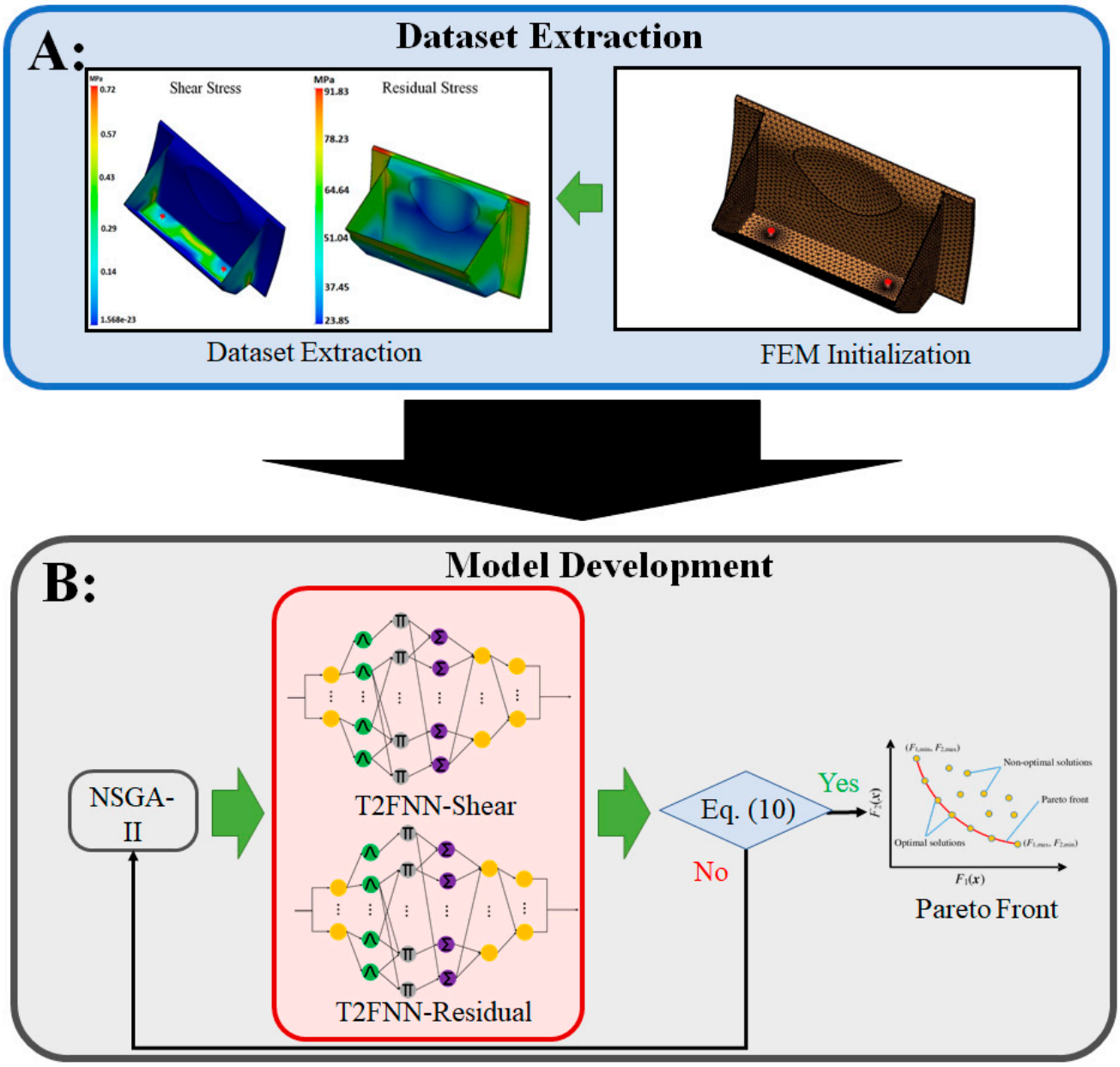

Figure 3. The overview of the proposed method in this study for extracting the optimal injection moulding process parameter for dashboard production (**A**) data extraction; (**B**) modelling and optimisation.

Concluding the data preprocessing stage involves partitioning the dataset into distinct training and testing samples. For this study, 80% of the dataset is allocated for training. The remaining 20% is reserved for testing the network's performance.

3.2. Type-2 Fuzzy Neural Network

T2FNN emerges as a powerful fusion, integrating a neural network and a type-2 FIS to achieve optimal tuning. Within this study, the type-2 FIS takes centre stage, meticulously calculating both shear and residual stress in the injection moulding process. These

individual components, denoted as T2FNN-Shear and T2FNN-Residual, respectively, harmoniously collaborate to deliver accurate insights. Figure 4 artistically showcases the membership functions employed by the interval type-2 FIS. These functions have been strategically designed to effectively handle the intricacies associated with internal shear and residual stress. For this analysis, a set of captured datasets, conveniently arranged in Table 1, serves as the foundation for training and testing the proposed model.

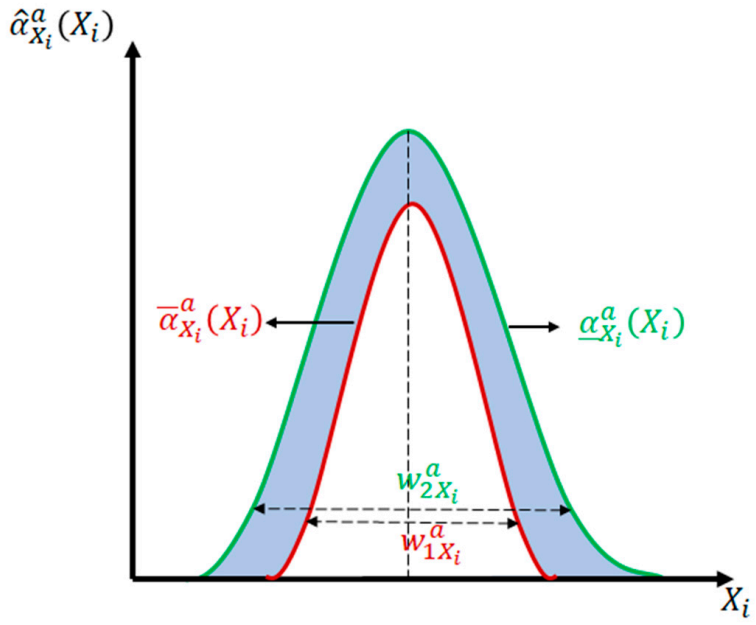

Figure 4. Membership function of the type-2 fuzzy interface.

Moreover, complementing the type-2 FIS model, a feedforward neural network has been seamlessly integrated. This addition contributes to fine-tuning the model, facilitating the precise calculation of internal shear and residual stress. The comprehensive structure of this hybrid T2FNN model is skilfully depicted in the captivating Figure 5.

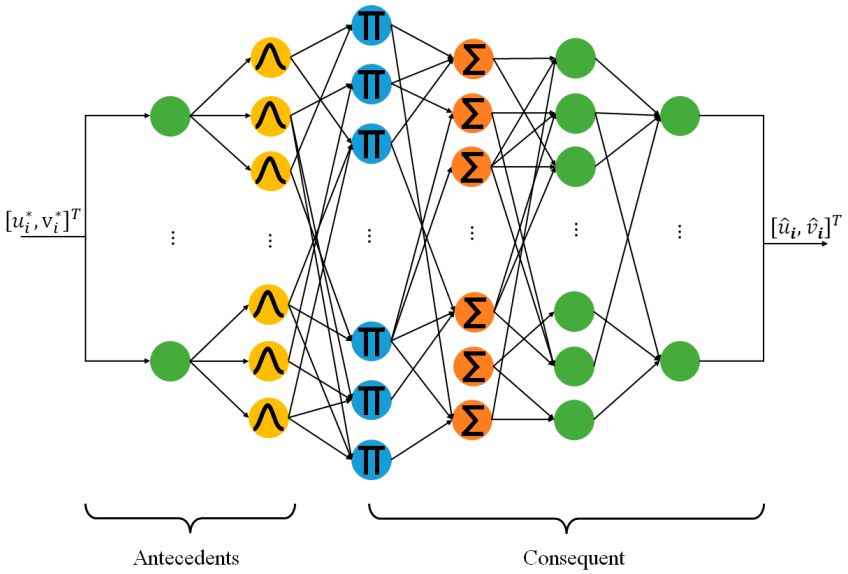

Figure 5. Schematic representation of the T2FNN.

The T2FNN involves the development of the considered system through the utilisation of multiple type-2 FIS IF-THEN rules, as outlined below:

$$\begin{aligned} &\textbf{Rule } \boldsymbol{a_i}: \textbf{ IF } \mathbf{u_i^*} \in \boldsymbol{Q_u^a} \textbf{ and } \mathbf{v_i^*} \in \boldsymbol{Q_v^a} \\ &\text{THEN}: \; X_i^a = \left[\mathrm{u}_i^{aT}, \mathrm{v}_i^{aT}\right]^T = \hat{r}_{i0}^a + \hat{R}_{u,v}^a \left[\mathrm{u}_i^{*T}, \mathrm{v}_i^{*T}\right]^T = \hat{r}_{i0}^a + \hat{R}_{u,v}^a X_i^* \end{aligned} \tag{2}$$

where

$$\hat{R}_{u,v}^a = \left[\hat{r}_{u,v,1}^a, \ldots, \hat{r}_{u,v,5}^a\right]^T \text{ while } \hat{r}_{u,v,n}^a \in \left[\underline{r}_{u,v,n}^a, \overline{r}_{u,v,n}^a\right],\ n = 1, \ldots, 5 \tag{3}$$

Moreover, u_i^* and v_i^* represent the reference signals, with a_i denoting the number of rules for systems i within the set $\{n, q\}$. Additionally, Q_u^a and Q_v^a comprise the sets of type-2 FISs, each equipped with their respective membership functions.

Therefore:

$$\begin{aligned} \underline{X}_i^a &= \underline{r}_{i0}^a + \underline{R}_{u,v}^a X_i^* \\ \overline{X}_i^a &= \overline{r}_{i0}^a + \overline{R}_{u,v}^a X_i^* \end{aligned} \tag{4}$$

Using the fuzzy sets illustrated in Figure 4 as a reference, we define $\hat{\alpha}_u^a(\mathrm{v}_i) = [\underline{\alpha}_u^a(\mathrm{v}_i), \overline{\alpha}_u^a(\mathrm{v}_i)]$ and $\hat{\alpha}_u^a(\mathrm{u}_i) = [\underline{\alpha}_u^a(\mathrm{u}_i), \overline{\alpha}_u^a(\mathrm{u}_i)]$ as uncertain standard deviation and mean Gaussian functions, while:

$$0 \le \underline{\alpha}_{X_i}^a(X_i) \le \overline{\alpha}_{X_i}^a(X_i) \le 1 \tag{5}$$

and

$$\begin{aligned} \underline{\alpha}_{X_i}^a(X_i) &= e^{\left(-\frac{1}{2}\left(\frac{X_i - c_{X_i}^a}{w_{1X_i}^a}\right)^2\right)} \\ \overline{\alpha}_{X_i}^a(X_i) &= e^{\left(-\frac{1}{2}\left(\frac{X_i - c_{X_i}^a}{w_{2X_i}^a}\right)^2\right)} \end{aligned} \tag{6}$$

By multiplying the type-2 fuzzy sets, the final outputs of the fuzzy rules in each system are determined in the following manner:

$$\begin{aligned} \underline{\mu}_{X_i}^a(X_i) &= \underline{\alpha}_u^a(\mathrm{u}_i) \times \underline{\alpha}_u^a(\mathrm{v}_i) \\ \overline{\mu}_{X_i}^a(X_i) &= \overline{\alpha}_u^a(\mathrm{u}_i) \times \overline{\alpha}_u^a(\mathrm{v}_i) \end{aligned} \tag{7}$$

So

$$\hat{X}_i = \frac{1}{2}\left(\frac{\sum_{a=1}^{A_i} \underline{\mu}_{X_i}^a(X_i)\underline{X}_i^a}{\sum_{a=1}^{A_i} \underline{\mu}_{X_i}^a(X_i)} + \frac{\sum_{a=1}^{A_i} \overline{\mu}_{X_i}^a(X_i)\overline{X}_i^a}{\sum_{a=1}^{A_i} \overline{\mu}_{X_i}^a(X_i)}\right) \tag{8}$$

The generation of parameters within the type-2 FIS is accomplished by training a neural network utilizing the datasets employed in this study. The fuzzy neural network, operating on the principles of the Takagi-Sugeno fuzzy structure, skilfully incorporates the represented rules outlined in Equation (3). Visualizing the intricate mechanism of the T2FNN is Figure 5, a captivating depiction illustrating the system's functionality through the arrangement of five layers or two distinct main groups, namely the antecedents and the consequents.

3.3. Multi-Objective Genetic Algorithm

In 1995, Deb et al. [29] proposed an innovative algorithm known as single objective GA, seamlessly merging genetic algorithms and Pareto optimisation to tackle the complexities of multi-objective optimisation problems. Building upon this foundation, in 2002, the MOGA emerged as a noteworthy enhancement, strategically designed to streamline system complexities and bolster solution calculation speed through individual stratification. One of the key advantages of MOGA lies in its remarkable ability to extract Pareto front solutions, even within the realm of non-convex problems. Remarkably, the computational efficiency of MOGA is underscored by the fact that the Pareto front distribution can be extracted in a single run. Delving into the inner workings of MOGA, the initial step revolves around calculating penalty values utilizing the proposed T2FNN models. Subsequently, the genetic

operator takes centre stage, employing mutation and crossover techniques to generate a new population. Embodying the essence of MOGA, the Elitist strategy meticulously selects the best solution from each newly generated population, effectively preserving the cream of the crop. This iterative process continues until the specified number of iterations is fulfilled. No definitive termination goal exists in the realm of MOGA, as the absence of a singular objective function necessitates alternative approaches. Combining crowding distance and non-domain sorting functions enables the cyclic grading essential to the algorithm's operation.

The initial step entails identifying the foremost non-dominated layer derived from the non-dominated set residing within the group. Subsequently, the said non-dominated set is promptly eliminated from the group, clearing the path for further exploration. The search endeavours persist within the remaining group, driving the process forward. Lastly, the solutions undergo a meticulous sorting procedure, meticulously arranged based on the intricacies of the dominance relationship.

Within this study, two objective functions are determined through the calculation of the mean square error (MSE) between the actual values acquired via finite element simulation and the predictions generated by the proposed T2FNN models:

$$\begin{aligned} J_{O1}(T_1, T_2, t_1, t_2) &= \frac{1}{n}\sum_{i=1}^{n}\left({\sigma^S}_i - {\hat{\sigma^S}}_i\right)^2 \\ J_{O2}(T_1, T_2, t_1, t_2) &= \frac{1}{n}\sum_{i=1}^{n}\left({\sigma^R}_i - {\hat{\sigma^R}}_i\right)^2 \end{aligned} \tag{9}$$

where σ^S and $\hat{\sigma^S}$ stand for actual and predicted internal shear stress via finite element simulation and the proposed T2FNN, respectively. In addition, σ^R and $\hat{\sigma^R}$ stand for actual and predicted internal stress residual via finite element simulation and the proposed T2FNN, respectively. Also, T_1, T_2, t_1, and t_2 are melt temperature, mould temperature, pressure holding time, and pure holding time, respectively.

The computation of inter-solution distances is undertaken by employing the crowding distance technique, thereby facilitating the density determination of the neighbouring solutions. This involves summing the distances between the individuals for each objective function. Additionally, normalisation is implemented as a preventive measure to address the issue of varying scales between objectives.

4. Results

The proposed technique is initially formulated and implemented within the MATLAB environment, as Section 3 outlines. These variants are denoted as T2FNN-Residual and T2FNN-Shear, and they forecast residual and shear stress for the end product of injection moulding. The predictive models rely on the manipulation of process parameters, namely T_1 (°C), T_2 (°C), t_1 (s), and t_2 (s). Given the adjustable nature of these process parameters, they are all incorporated in the derivation of the optimal solution, ensuring the attainment of a final product with superior mechanical attributes. A total of 80% of the provided datasets (144 sets) are utilised for training the networks. In comparison, the remaining 20% (36 sets) are reserved for testing the model.

Figure 6a,b illustrates the correlations between the outcomes derived from finite element analysis and the forecasts generated for residual and shear stress. This evaluation encompasses the entire datasets, encompassing training and testing subsets, utilizing T2FNN-Residual and T2FNN-Shear models. As indicated in Figure 6a, the predictive performance of T2FNN-Residual in estimating residual stress exhibits correlation coefficients of 0.9777 and 0.9868 for the training and testing datasets, respectively. Similarly, Figure 6b illustrates a distinct pattern, where the regression coefficients for T2FNN-Residual in the domain of residual stress prediction are 0.9731 and 0.5671 for the training and testing datasets correspondingly. Regarding computational efficiency, the training durations for T2FNN-Residual and T2FNN-Shear, executed on a computer equipped with Intel(R) Core(TM) i7-10875H CPU @ 2.30 GHz 2.30 GHz, amount to 1.609482 and 3.605136 s, respectively.

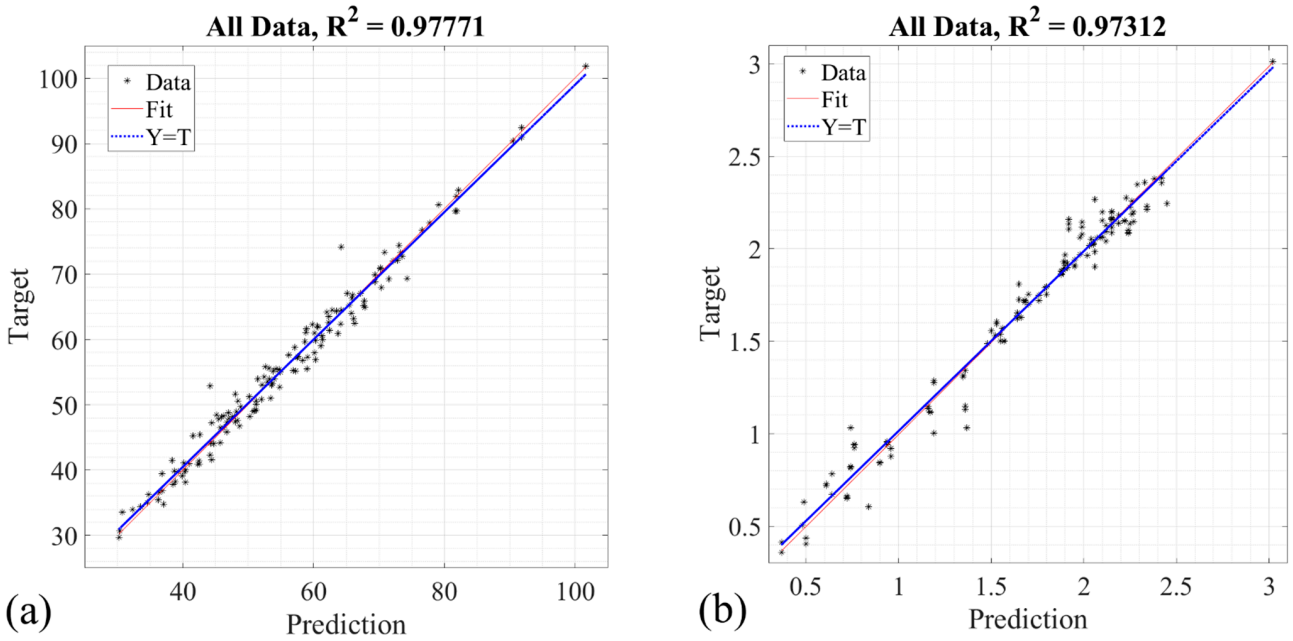

Figure 6. The regression of the whole dataset (training and testing) using (**a**) T2FNN-Residual for prediction of the residual stress; (**b**) T2FNN-Shear for prediction of the shear stress.

Figure 7a,b displays residual and shear stress assessment within the dashboard's final product. This appraisal involves employing both the finite element framework and the suggested T2FNN-Residual and T2FNN-Shear models during the testing phase of the network. The finite element results serve as the benchmark against which the outcomes of T2FNN-Residual and T2FNN-Shear are juxtaposed, facilitating an evaluation of the proposed models' precision. Figure 7a delineates the computation of residual stress for 36 testing samples, utilizing both the finite element environment and T2FNN-Residual. As evidenced by the findings in Figure 7a, the correlation coefficient between the finite element outcomes and the projected residual stress yielded by the proposed T2FNN-Residual model amounts to 0.9848. Furthermore, Figure 7b demonstrates that, encompassing 44 testing samples, the correlation coefficient between the finite element results and the projected shear stress generated by the suggested T2FNN-Shear model stands at 0.7349.

Figure 8a,b illustrates the discrepancy between the anticipated and reference (finite element) values for both residual and shear stress predictions, employing the T2FNN models. Analysing the outcomes depicted in Figure 8a, it becomes evident that the mean square error between the predicted and finite element-based residual stress, as determined by the proposed T2FNN-Torque, equates to 6.8829 (MPa). Similarly, in the ensuing analysis, the mean square error about the anticipated and finite element-based shear stress, facilitated by the newly developed T2FNN-Shear model, computes to 0.1546 (MPa), as reflected in Figure 8b. Additionally, the root mean square errors, gauged between the predicted and finite element-derived residual and shear stress, are 2.6235 and 0.3932 (MPa), respectively, following the data portrayed in Figure 8a,b. Lastly, assessing the normalised root mean square errors, it is deducible that T2FNN-Residual boasts superior predictive accuracy compared to T2FNN-Shear, given its lower value of 0.0482 in contrast to 0.2263 (MPa) as delineated in Figure 8a,b.

All the represented results in Figures 6–8 are shown in Table 2 for a quick check of the proposed method's performance. The concepts of mean square error, root means square error, normalised root means square error, correlation coefficient, r-square, mean of error, and standard deviation of error are used to show the efficiency of the proposed method.

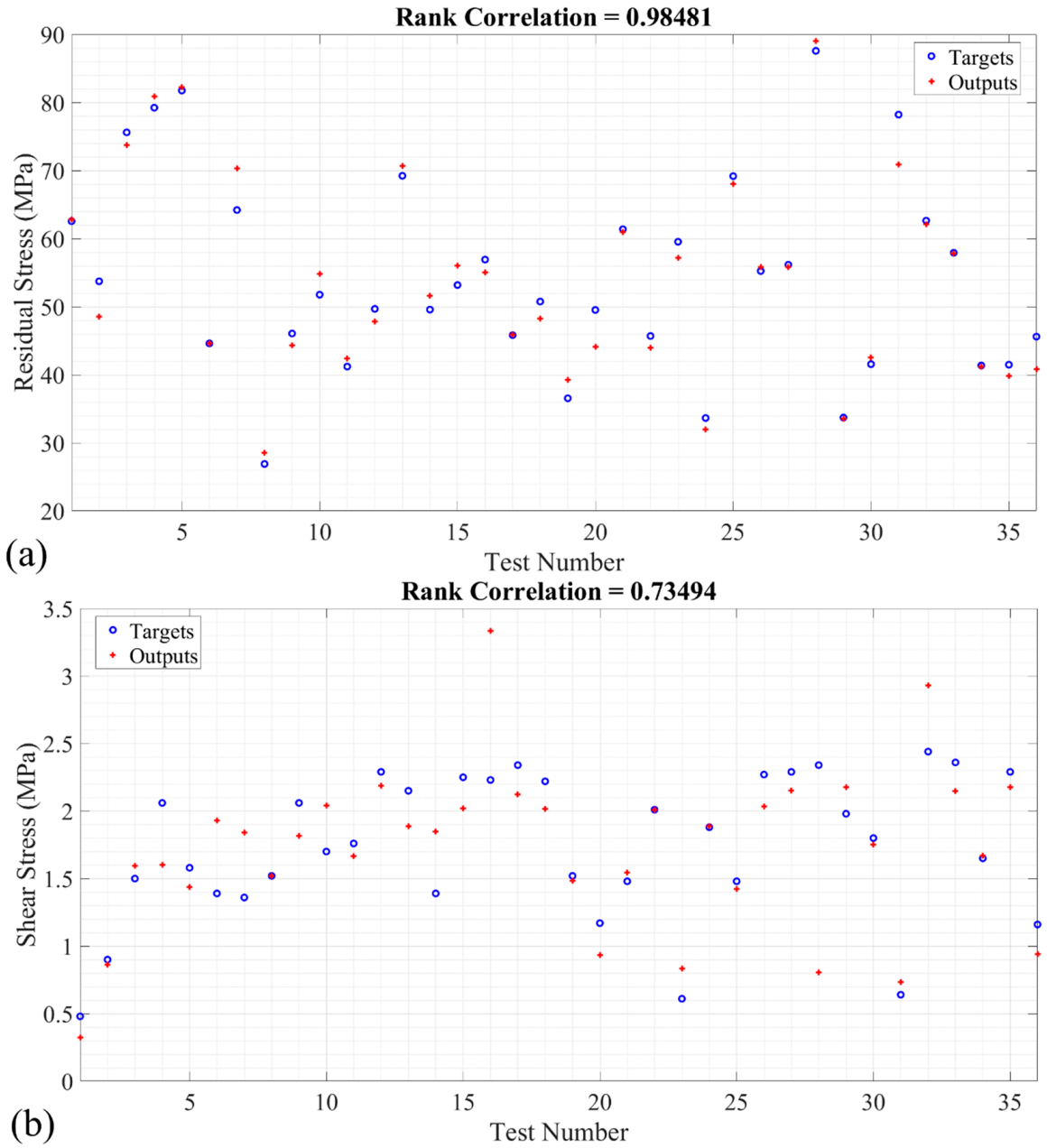

Figure 7. The finite element and predicted residual and shear stress using (**a**) T2FNN-Residual; (**b**) T2FNN-Shear.

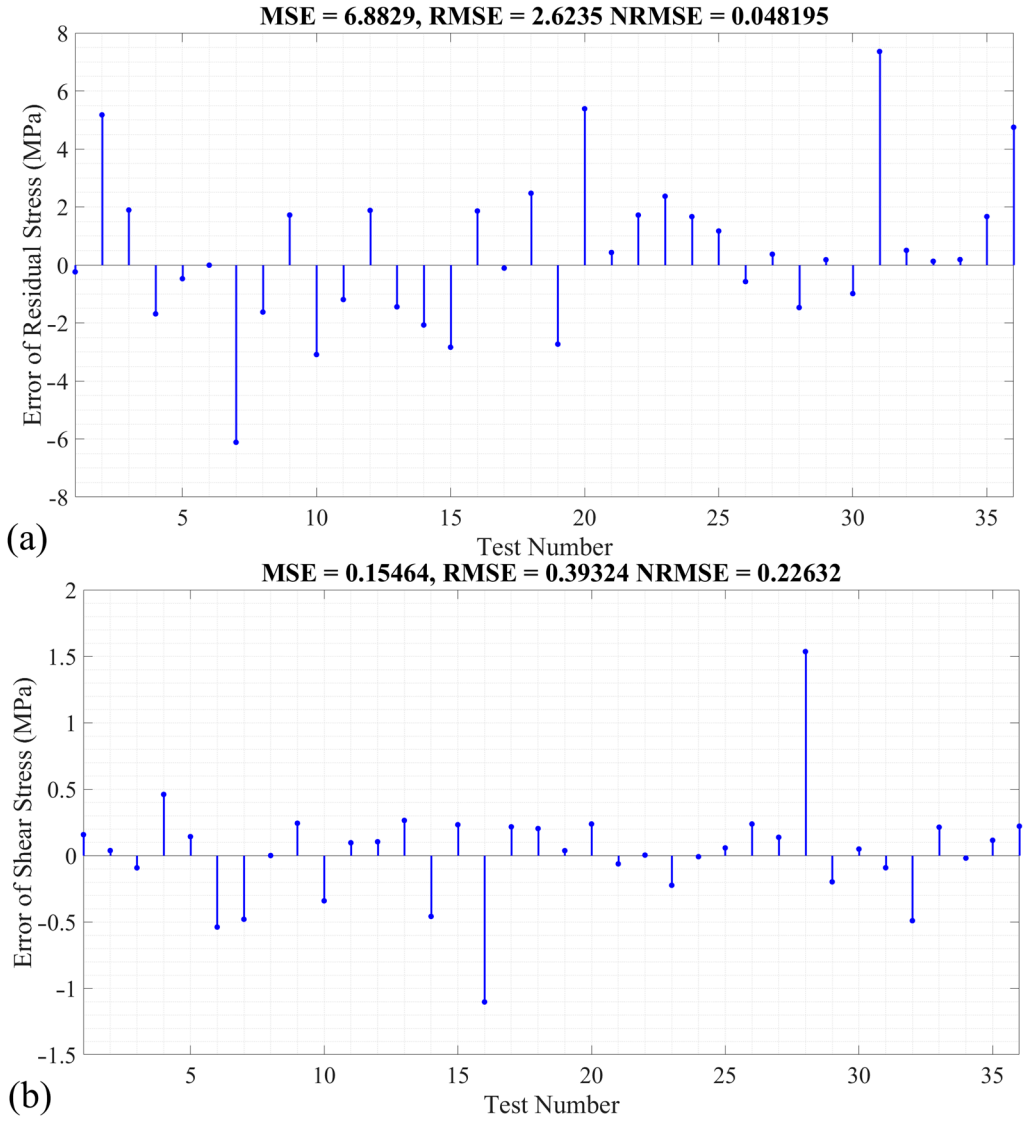

Figure 8. The error between the finite element and predicted value using the proposed T2FNN models to predict (**a**) residual stress; (**b**) shear stress.

Table 2. The extracted results for investigation of implementing T2FNN-Residual and T2FNN-Shear for calculation of residual and shear stress based on T_1, T_2, t_1, and t_2 (MSE: mean square error; RMSE: root means square error; NRMSE: normalised root mean square error; CC: correlation coefficient; R^2: R-square).

Index	T2FNN-Residual			T2FNN-Shear		
	Training	Testing	All	Training	Testing	All
MSE	4.1436	6.8829	4.1436	8.47×10^{-3}	1.55×10^{-1}	8.47×10^{-3}
RMSE	2.0356	2.6235	2.0356	9.20×10^{-2}	3.93×10^{-1}	9.20×10^{-2}
NRMSE	0.0366	0.0482	0.0366	5.54×10^{-2}	2.26×10^{-1}	5.54×10^{-2}
CC	0.9868	0.9848	0.9868	0.9758	0.7349	0.9758
R^2	0.9777	0.9680	0.9777	0.9731	0.5671	0.9731
Mean of error	−0.1217	0.4515	−0.1217	3.29×10^{-3}	2.43×10^{-2}	3.29×10^{-3}
Error std	2.039	2.621	2.039	9.23×10^{-2}	3.98×10^{-1}	9.23×10^{-2}

Figure 9a–d shows the rule surface of the extracted T2FNN-Residual and T2FNN-Shear in calculating the residual and shear stress based on different arrangements of the input process parameters, respectively. Figure 9a,b represents the system's behaviour (T2FNN-Residual) on the calculation residual stress based on the variation of T_1/T_2 and t_1/t_2, respectively. Figure 9a shows that T_1 (melt temperature) influences the final product's residual stress variation. The second effective input process parameter in the residual stress variation is T_2 (mould temperature). t_2 (pressure cooling time) and t_1 (pressure holding time) can be categorised as the third and fourth levels of influence parameters in the residual stress of the final product. However, the influence of T_1 (melt temperature) and T_2 (mould temperature) on the variation in shear stress are reported as the same based on the represented results in Figure 9c. It also shows the same influence for the t_2 (pressure cooling time) and t_1 (pressure holding time) in the variation in shear stress (Figure 9d). As a result, T_1 and T_2 are the first effective parameters in the variation in shear stress, which put the t_1 and t_2 in the second level of influence.

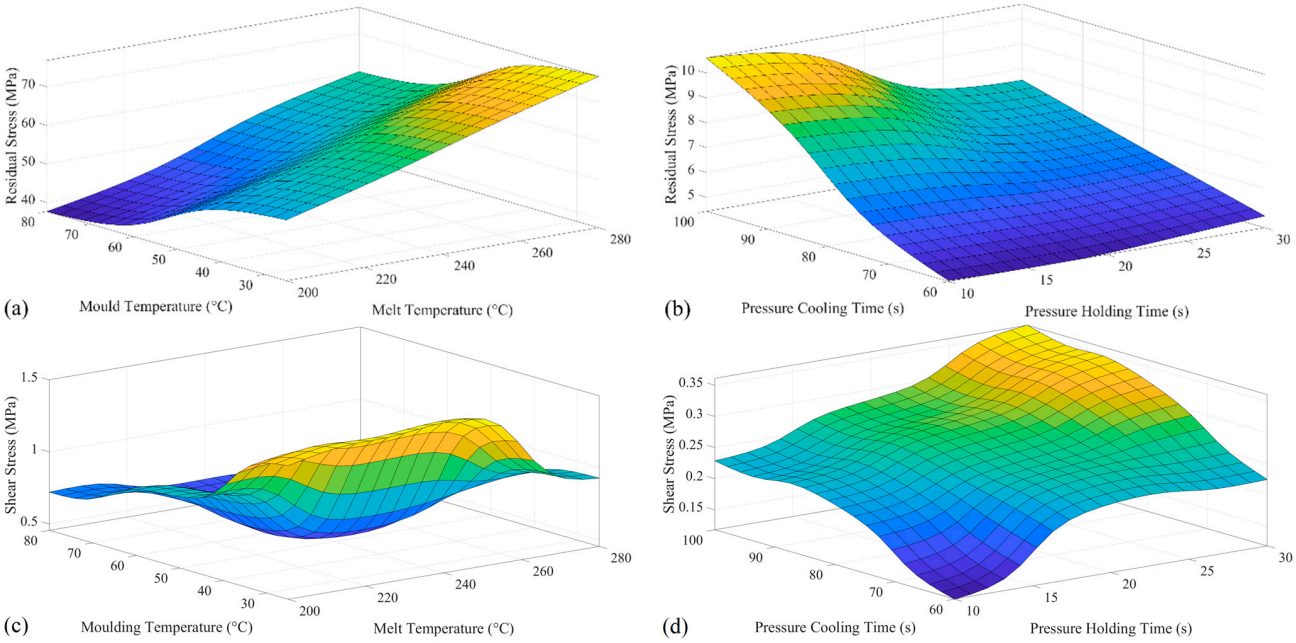

Figure 9. T2FNN rule surface for the calculation of (**a**) residual stress using T_1 and T_2; (**b**) residual stress using t_1 and t_2; (**c**) shear stress using T_1 and T_2; (**d**) shear stress using t_1 and t_2.

Subsequently, the application of the T2FNN models for forecasting residual and shear stress is integrated into the MOGA framework, aimed at deducing the optimal set of process parameters for the injection moulding process. The Pareto front distribution, characterizing the optimal process solutions, is displayed in Figure 10. In contrast, the corresponding optimal solutions are outlined in Table 3. A series of finite element experiments were conducted to validate the system's accuracy, guided by the extracted optimal solutions derived from the proposed T2FNN and MOGA approaches. A comprehensive comparison was then undertaken, contrasting the experimental outcomes with those generated by the proposed T2FNN and MOGA, as showcased in the final column of Table 3. The results distinctly manifest an impressive alignment between the proposed method and the experimental data, revealing a marginal nonconformance of less than 8.28%. This substantiates the precision of the proposed approach in prognosticating residual and shear stress within the injection moulding process for dashboards.

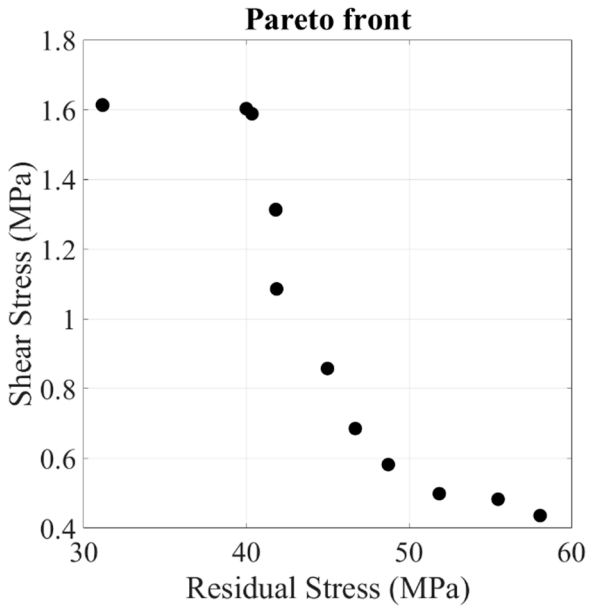

Figure 10. Pareto front of the extracted optimal solution using MOGA in the injection moulding process to extract the optimal residual and shear stress.

Table 3. Extracted optimal process parameters of the injection moulding process of the dashboard using T2FNN models and MOGA.

No.	T_1 (°C)	T_2 (°C)	t_1 (seconds)	t_2 (seconds)	Error %
1	246.141	75.058	11.291	76.775	2
2	244.166	75.187	11.327	72.615	8
3	208.649	77.260	13.654	69.917	5
4	210.981	77.144	15.019	69.763	16
5	226.885	75.322	11.397	73.876	9
6	233.623	75.225	11.347	75.182	18
7	246.141	75.058	11.291	76.775	4
8	209.384	77.255	16.903	70.048	5
9	220.384	76.748	12.881	70.162	3
10	208.649	77.418	17.137	70.078	3
11	210.983	77.144	15.024	69.771	17
12	207.830	77.438	29.127	69.619	12
13	224.537	75.682	11.934	70.834	11
14	207.863	77.447	29.033	69.434	3

5. Discussion

This study proposed a method to enhance the injection moulding process by minimizing various plastic defects such as shear stress, and residual stress in the final product. It introduces a structured framework for optimizing process parameters like temperature, pressure, and speed, crucial for achieving high-quality results in injection moulding. The method offers a novel approach, distinct from conventional methods, with potential advantages in terms of efficiency and effectiveness. Sensitivity analysis is performed in this study to evaluate how changes in input parameters affect outcomes by identifying the areas of concern and guiding adjustments to improve the accuracy of the analysis. Also, through rigorous experimentation, the study validates the effectiveness of this method

in reducing plastic defects, thereby bolstering its credibility [30]. Additionally, while the research primarily addresses specific defects, it hints at the method's adaptability to other defect types, indicating its broader applicability. Furthermore, the study suggests avenues for future research to explore the method's potential enhancements and its application to other defect categories, underscoring its significance for ongoing research in the field.

6. Conclusions

The study examined injection moulding to evaluate plastic product properties, focusing on shear and residual stresses. Key variables were selected, and a factorial experiment identified optimal settings. Computational techniques, like finite element analysis, assessed input impacts. The novel approach integrated T2FNN and MOGA to model and optimise injection moulding. Validation used a CAD model. Investigation results highlighted process variables impacting properties, e.g., melt/mould temperature, pressure holding time, and pressure cooling time. T2FNN estimated stresses accurately, improving modelling with process uncertainties. T2FNN combined with MOGA extracted optimal parameters, reducing shear and residual stress and enhancing product resistance. Finite element simulation proved efficient in dataset generation, avoiding costly experiments. The T2FNN-MOGA combination excelled in optimizing complex systems like injection moulding. The hybrid model determined Pareto-optimal solutions, enhancing plastic manufacturing efficiency. Study contributions were twofold: novel T2FNN use for stress estimation and MOGA incorporation for process optimisation. Implications for plastic manufacturing include quality improvement, defect reduction, and process efficiency enhancement. Findings hold the potential to significantly impact the injection moulding field.

Author Contributions: Conceptualisation, M.M.; data curation, P.J.A., M.H.-D., A.A. (Ahmed Abdalmonem), A.A. (Ahmad Alsmadi) and F.A.; formal analysis, M.R.C.Q. and M.M.; investigation, M.M.; methodology, M.R.C.Q. and M.M.; resources, M.M., M.H.-D., A.A. (Ahmed Abdalmonem) and A.A. (Ahmad Alsmadi); software, M.R.C.Q., M.M. and P.J.A.; supervision, M.R.C.Q. and M.M.; validation, M.R.C.Q. and M.M.; visualisation, M.R.C.Q., P.J.A. and F.A.; writing—original draft, M.R.C.Q. and M.M.; writing—review and editing, P.J.A., M.H.-D., A.A. (Ahmed Abdalmonem), A.A. (Ahmad Alsmadi) and F.A. All authors have read and agreed to the published version of the manuscript.

Funding: The authors declare that there is no funding to report regarding the present study.

Data Availability Statement: The datasets generated and/or analysed during the current study are available from the corresponding author upon reasonable request.

Conflicts of Interest: The authors declare that they have no known competing financial interests or personal relationships that could have appeared to influence the work reported in this paper.

References

1. Zhou, H. Part II: Simulation, Mathematical Models for the Filling and Packing Simulation. In *Computer Modeling for Injection Molding*; John Wiley & Sons, Inc.: Hoboken, NJ, USA, 2013; pp. 49–254.
2. Bozdana, A.T.; Eyercïoğlu, Ö. Development of an expert system for the determination of injection moulding parameters of thermoplastic materials: EX-PIMM. *J. Mater. Process. Technol.* **2002**, *128*, 113–122. [CrossRef]
3. Moayyedian, M.; Abhary, K.; Marian, R. The analysis of short shot possibility in injection molding process. *Int. J. Adv. Manuf. Technol.* **2017**, *91*, 3977–3989. [CrossRef]
4. Youssef, Y.; Denault, J. Thermoformed glass fiber reinforced polypropylene: Microstructure, mechanical properties and residual stresses. *Polym. Compos.* **1998**, *19*, 301–309. [CrossRef]
5. Gere, J.M.; Goodno, B.J. *Mechanics of Materials*; Cengage Learning: Boston, MA, USA, 2012.
6. Chuong, C.-J.; Fung, Y.-C. Residual stress in arteries. In *Frontiers in Biomechanics*; Springer: Berlin/Heidelberg, Germany, 1986; pp. 117–129.
7. Schwetz, K.A.; Sigl, L.S.; Pfau, L. Mechanical properties of injection molded B4C–C ceramics. *J. Solid State Chem.* **1997**, *133*, 68–76. [CrossRef]
8. Torres, N.; Robin, J.; Boutevin, B. Study of thermal and mechanical properties of virgin and recycled poly (ethylene terephthalate) before and after injection molding. *Eur. Polym. J.* **2000**, *36*, 2075–2080. [CrossRef]
9. Ozcelik, B.; Ozbay, A.; Demirbas, E. Influence of injection parameters and mold materials on mechanical properties of ABS in plastic injection molding. *Int. Commun. Heat Mass Transf.* **2010**, *37*, 1359–1365. [CrossRef]

10. Kuzmanović, M.; Delva, L.; Cardon, L.; Ragaert, K. The effect of injection molding temperature on the morphology and mechanical properties of PP/PET blends and microfibrillar composites. *Polymers* **2016**, *8*, 355. [CrossRef]
11. Krantz, J.; Nieduzak, Z.; Kazmer, E.; Licata, J.; Ferki, O.; Gao, P.; Sobkowicz, M.J.; Masato, D. Investigation of pressure-controlled injection molding on the mechanical properties and embodied energy of recycled high-density polyethylene. *Sustain. Mater. Technol.* **2023**, *36*, e00651. [CrossRef]
12. Chin, K.-S.; Wong, T. Knowledge-based evaluation for the conceptual design development of injection molding parts. *Eng. Appl. Artif. Intell.* **1996**, *9*, 359–376. [CrossRef]
13. Kenig, S.; Ben-David, A.; Omer, M.; Sadeh, A. Control of properties in injection molding by neural networks. *Eng. Appl. Artif. Intell.* **2001**, *14*, 819–823. [CrossRef]
14. Tan, K.; Tang, J. Learning-enhanced PI control of ram velocity in injection molding machines. *Eng. Appl. Artif. Intell.* **2002**, *15*, 65–72. [CrossRef]
15. Abbasalizadeh, M.; Hasanzadeh, R.; Mohamadian, Z.; Azdast, T.; Rostami, M. Experimental study to optimize shrinkage behavior of semi-crystalline and amorphous thermoplastics. *Iran. J. Mater. Sci. Eng.* **2018**, *15*, 41–51.
16. Abdul, R.; Guo, G.; Chen, J.C.; Yoo, J.J.-W. Shrinkage prediction of injection molded high density polyethylene parts with taguchi/artificial neural network hybrid experimental design. *Int. J. Interact. Des. Manuf.* **2020**, *14*, 345–357. [CrossRef]
17. Song, Z.; Liu, S.; Wang, X.; Hu, Z. Optimization and prediction of volume shrinkage and warpage of injection-molded thin-walled parts based on neural network. *Int. J. Adv. Manuf. Technol.* **2020**, *109*, 755–769. [CrossRef]
18. Gao, Z.; Dong, G.; Tang, Y.; Zhao, Y.F. Machine learning aided design of conformal cooling channels for injection molding. *J. Intell. Manuf.* **2021**, *34*, 1183–1201. [CrossRef]
19. Jung, H.; Jeon, J.; Choi, D.; Park, J.-Y. Application of Machine Learning Techniques in Injection Molding Quality Prediction: Implications on Sustainable Manufacturing Industry. *Sustainability* **2021**, *13*, 4120. [CrossRef]
20. Uğuroğlu, E. Near-Real Time Quality Prediction in a Plastic Injection Molding Process Using Apache Spark. In Proceedings of the 2021 International Symposium on Computer Science and Intelligent Controls (ISCSIC), Rome, Italy, 12–14 November 2021; pp. 284–290.
21. Párizs, R.D.; Török, D.; Ageyeva, T.; Kovács, J.G. Machine Learning in Injection Molding: An Industry 4.0 Method of Quality Prediction. *Sensors* **2022**, *22*, 2704. [CrossRef]
22. Ke, K.-C.; Huang, M.-S. Enhancement of multilayer perceptron model training accuracy through the optimization of hyperparameters: A case study of the quality prediction of injection-molded parts. *Int. J. Adv. Manuf. Technol.* **2022**, *118*, 2247–2263. [CrossRef]
23. Moayyedian, M.; Qazani, M.R.C.; Pourmostaghimi, V. Optimized injection-molding process for thin-walled polypropylene part using genetic programming and interior point solver. *Int. J. Adv. Manuf. Technol.* **2023**, *124*, 297–313. [CrossRef]
24. Gim, J.; Yang, H.; Turng, L.-S. Transfer learning of machine learning models for multi-objective process optimization of a transferred mold to ensure efficient and robust injection molding of high surface quality parts. *J. Manuf. Process.* **2023**, *87*, 11–24. [CrossRef]
25. Fernández-León, J.; Keramati, K.; Miguel, C.; González, C.; Baumela, L. A deep encoder-decoder for surrogate modelling of liquid moulding of composites. *Eng. Appl. Artif. Intell.* **2023**, *120*, 105945. [CrossRef]
26. Zhang, Z.; Zhou, M.; Wan, H.; Li, M.; Li, G.; Han, D. IDD-Net: Industrial defect detection method based on Deep-Learning. *Eng. Appl. Artif. Intell.* **2023**, *123*, 106390. [CrossRef]
27. Moayyedian, M.; Dinc, A.; Mamedov, A. Optimization of injection-molding process for thin-walled polypropylene part using artificial neural network and Taguchi techniques. *Polymers* **2021**, *13*, 4158. [CrossRef]
28. Goodsgip, V. *Troubleshooting Injection Moulding*; iSmithers Rapra Publishing: Shrewsbury, UK, 2004; Volume 15.
29. Deb, K. Real-coded genetic algorithms with simulated binary crossover: Studies on multimodal and multiobjective problems. *Complex Syst.* **1995**, *9*, 431–454.
30. Moayyedian, M. *Intelligent Optimization of Mold Design and Process Parameters in Injection Molding*; Springer: Berlin/Heidelberg, Germany, 2018.

Disclaimer/Publisher's Note: The statements, opinions and data contained in all publications are solely those of the individual author(s) and contributor(s) and not of MDPI and/or the editor(s). MDPI and/or the editor(s) disclaim responsibility for any injury to people or property resulting from any ideas, methods, instructions or products referred to in the content.